Structure and Crystallization Behavior of the β Phase of Oleic Acid

Fumitoshi Kaneko,* Kazuhiro Yamazaki, Kenji Kitagawa, Takashi Kikyo, and Masamichi Kobayashi

Department of Macromolecular Science, Graduate School of Science, Osaka University, Toyonaka, Osaka 560, Japan

Yasuyuki Kitagawa and Yoshiki Matsuura

Institute for Protein Research, Osaka University, Suita, Osaka 565, Japan

Kiyotaka Sato

Laboratory of Chemical Physics, Faculty of Applied Biological Science, Hiroshima University, Higashihiroshima, Hiroshima 724, Japan

Masao Suzuki

Oleochemical Research Laboratory, NOF Corporation, Ohama, Amagasaki, Hyogo 660, Japan

Received: October 31, 1996; In Final Form: January 14, 1997[⊗]

Crystallization and crystal structure of the β phase of oleic acid (*cis*-9-octadecenoic acid) have been investigated with morphological observation, X-ray diffraction, and DSC (differential scanning calorimeter). The morphology of growing crystals of the β phase depends significantly on supercooling. It was found that the β phase could be classified into at least two solid modifications, β_1 (mp 16.3 °C) and β_2 (mp 16.0 °C). The crystal structure analysis of the β_1 phase has been performed. The unit cell belongs to a triclinic system of $P\bar{1}$, and the asymmetric unit contains two crystallographically independent molecules, A and B. The molecular layer is a unique interdigitated structure, where the methyl group of molecule A and the carboxyl group of molecules B (or vice versa) are located on the same plane. For the conformation around the cis-C=C bond, both molecules approximate to trans−cis−trans conformation, the first case for a cis-monounsaturated fatty acid. The methyl and carboxyl side chains together form a T|| subcell. On the basis of its crystal structure, it was speculated that the β_1 phase has a unique surface structure at the (001) face. The factors for the characteristic properties of the β phase were also discussed.

Introduction

Unsaturated fatty acids are attracting considerable attention from various fields of science and technology. The use of unsaturated fatty acids and their derivatives has been becoming significantly important in the field of pharmaceutical, food, and cosmetic industries.

The functional activity of biological membranes is dependent on the amount and type of unsaturated fatty acids in phospholipids. The major part of phospholipids in biomembranes contains a saturated fatty acid and a cis-unsaturated fatty acid at the first and second positions of glycerol skeletons. Recent studies on phospholipids containing one unsaturated chain clarified that unsaturated acyl chains disturb stable close-packed structures of acyl chains, and therefore, many metastable states are generated.[1−4] Through a series of polymorphic studies on cis-unsaturated fatty acids, we have clarified that cis-unsaturation brings about great diversity in molecular conformation and packing.

Oleic acid (*cis*-9-octadecenoic acid) is the most abundant cis-unsaturated fatty acid in nature; it is distributed in almost all organisms. Therefore, the information about its molecular level structures and properties is fundamental to understand the behavior of unsaturated chains in biological systems and industrial products. Polymorphism, a phenomenon in which a compound forms different crystal structures by changing molecular conformation or aggregation state depending on conditions, reflects sensitively the structure and dynamical property of a compound. Through structural chemical studies on each polymorphic phase, we could understand the relationship between molecular and crystal structures and physicochemical properties.

Impurities have a large influence on the polymorphic behavior of long-chain compounds. Although samples of high purity are necessary to obtain faithful results, high-purity products of cis-unsaturated fatty acids have not been obtained. About a decade ago ultrapure oleic acid sample (guaranteed more than 99.9%) was produced with modern purification technology. Using this sample, we have studied the polymorphism of oleic acid,[5] confirming the presence of the three polymorphic phases, α, β, and γ, as shown in Figure 1. The γ and β phases correspond to the already known low-melting and high-melting phases,[6] and the former structure has already been determined.[7] The γ phase transforms to the α phase reversibly at −2.2 °C on heating, accompanying a selective conformational disordering in the methyl terminal chains.[8] The $\gamma \rightarrow \alpha$ solid-state phase transition has been found in other cis-monounsaturated fatty acids: palmitoleic acid, erucic acid, gondoic acid, and asclepic acid.[9−13]

The β phase is unique in the polymorphism of cis-monounsaturated fatty acids: in contrast to the α and γ phases, it has been found only in oleic acid and does not show an order−disorder type solid-state phase transition like the $\gamma \rightarrow \alpha$

[⊗] Abstract published in *Advance ACS Abstracts,* February 15, 1997.

S1089-5647(96)03400-1 CCC: $14.00

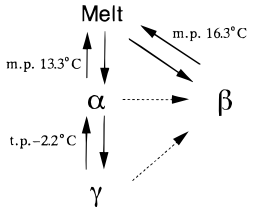

Figure 1. Polymorphism of oleic acid. Solid and broken lines represent reversible and irreversible processes, respectively.

transition. Only irreversible transitions to the β phase have been confirmed: a very slow solid-state irreversible transition from α and solution-mediated transitions from α and γ. The crystallization behavior of the β phase is also unique.[14,15] The growth rate is quite slow compared with the other polymorphic phases of cis-monounsaturated fatty acids. In melt crystallization at a supercooling of 0.5 °C, the growth rate of the β phase is ca. 10^5 times slower than that of the α phase. Such a remarkable difference among polymorphic phases has not been reported so far.

The powder X-ray reflection pattern of the β phase suggests a peculiar crystal structure. Polymorphic phases of fatty acids (except the A_1 and A-super forms of lauric acid) form a layered structure whose lamellar interface consists of methyl terminals. This layered structure makes a clear periodical contrast of electron density along the lamellar stacking direction: a low-density region of methyl terminals and a high-density region of dimerizing carboxyl terminals. The clear contrast results in intense reflections assigned to long spacings for $2\theta < 10°$. Indeed, the α and γ phases of oleic acid exhibit intense reflections of long spacings. However, only several weak reflections are observed in the same range for the β phase, which cannot be interpreted with the layered structure where methyl and carboxyl groups are segregated from each other.

Experimental results described above indicate that the difference in the aggregation state changes the physicochemical properties remarkably. In this study, we investigate the crystallization process of the β phase and its crystal structure. At first, we describe that the β phase can be classified into two modifications: stable β_1 and metastable β_2. Next we show the unique molecular conformation and aggregation state in the crystal structure of the β_1 phase. We also discuss the factors affecting the physicochemical properties specific to the β phase.

Experimental Section

Materials. Ultrapure oleic acid (purity > 99.9%) was supplied from NOF Corporation. Acetonitrile (>99% purity, Nakarai Tesque) was employed as solvent for growing single crystals, which were used for X-ray crystal structure analysis.

Microscopic Observation. Crystal growth of oleic acid was observed with a transmission type Normarsky interference contrast microscopy (Olympus IMT2-NIC). The temperature was measured with a copper−constantan thermocouple. The temperature of a glass cell for microscopic observation was controlled within ±0.05 °C by circulating water from a thermostat (Tokyo-Rika).

For the observation of crystals of β that spontaneously occur, a melt of β was kept at 17.0 °C about 10 min and cooled to 10−11 °C. Usually, the crystallization of β started within 1 h. Then the specimen was heated to a certain temperature for morphology observation (parts a−c of Figures 2).

A small seed crystal of β was also used (Figures 2d and 3). At first a single crystal β was melted to several microns at 16.3 °C, and then it was cooled to a certain temperature.

The rate of temperature change for the above procedures was 0.3−0.5 °C/min.

DSC Measurement. DSC (differential scanning calorimeter) measurement was performed with Seiko Denshi DSC system (Model 5200). Samples (10 mg) were sealed in aluminum pans. The DSC data were taken between −20 and 30 °C with a heating rate of 2.0 °C/min.

Powder X-ray Diffraction. A powder X-ray diffraction pattern was taken with a Rigaku-Denki diffractometer with Cu Kα radiation monochromatized with a graphite monochromator. Samples were cooled at about −10 °C with a Rigaku-Denki cryostat.

X-ray Crystal Structure Analysis. A plate crystal of dimensions 0.7 × 0.5 × 0.2 mm^3 was used for intensity measurements. Specimens were cooled with a stream of dry air. Intensity data were obtained with a Rigaku-Denki AFC-5 automated four-circle diffractometer with Ni-filtered Cu Kα radiation from a rotating anode. Unit cell parameters were refined using the 2θ values of 24 reflections in the range $19 < 2\theta < 24°$. Reflections with $4 < 2\theta < 120°$ ($-10 < h < 10$, $0 < k < 6$, $-38 < l < 39$) were measured with ω-scan mode with a scan speed of 3 deg min^{-1}. The scan range is (1.6−0.1 tan θ)°. A total of 4593 reflections were collected. A quantity of 2873 observed reflections with the criterion of $I > 2\sigma(I)$ were used in the refinement. No absorption correction was performed. The initial coordinates of 20 carbon atoms were located by using the program SHELXS-93.[16] For least-squares calculations SHELXS-86[17] was used. The other atoms were located after several cycles of least-squares refinement and Fourier calculation. The initial coordinates of hydrogen atoms were geometrically calculated. The B factors of 68 hydrogen atoms were refined isotropically. $\sum w(I_o - I_c)^2$ was minimized. The weighting scheme is $w = 1/[\sigma(I_o)^2 + (0.1070P)]$ where $P = (I_o + 2I_c)/3$. A sample of 565 parameters were used for refinement. R_o is 0.057 and R_w is 0.155. $\Delta\max/\sigma$ is 0.089 and $\Delta\text{ave}/\sigma$ is 0.013. Atomic scattering factors were from *International Tables for X-ray Crystallography* (1974, Vol. IV). ORTEP II[18] was used for plotting the crystal structure.

Results

Growth Mechanism. On melt crystallization the morphology of the growing single crystals of β depends remarkably on supercooling. As shown in Figure 2a, the crystals of β do not have a definite shape below 13 °C. The β phase grows as an agglomerate of fine curved crystals. At about 14 °C crystals start to grow as straight serrated rod crystals (Figure 2b). At a slightly higher temperature triangle-shaped crystals appear at the lateral sides of the rod crystal (Figure 2c) and the lateral sides appears as a sawtooth. The sawtoothed edges become a straight line above 15.0 °C, and a ridge extending toward the growing crystal end appears in the center of the crystal face. This center ridge becomes obscured with increasing temperature, and single crystals tend to develop in the lateral direction. An isolated single-crystal exhibits a hexagon-shaped morphology at 15.5 °C (Figure 2d). These remarkable morphological changes (parts b−d of Figure 2) take place in a very narrow temperature range 14.1−15.5 °C, which is the phenomenon characteristic of the β phase.

Another important result is that the β phase can be divided into two phases slightly different from each other in melting point. Figure 3 shows the behavior on melting of oleic acid β. A rod-shaped crystal was retained at 15.5 °C. After a few minutes the center of the rod began to grow in the lateral direction (Figure 3a). When this crystal was heated from 15.5 to 16.1 °C with a rate of 0.3 °C/min, the lateral flat part melted

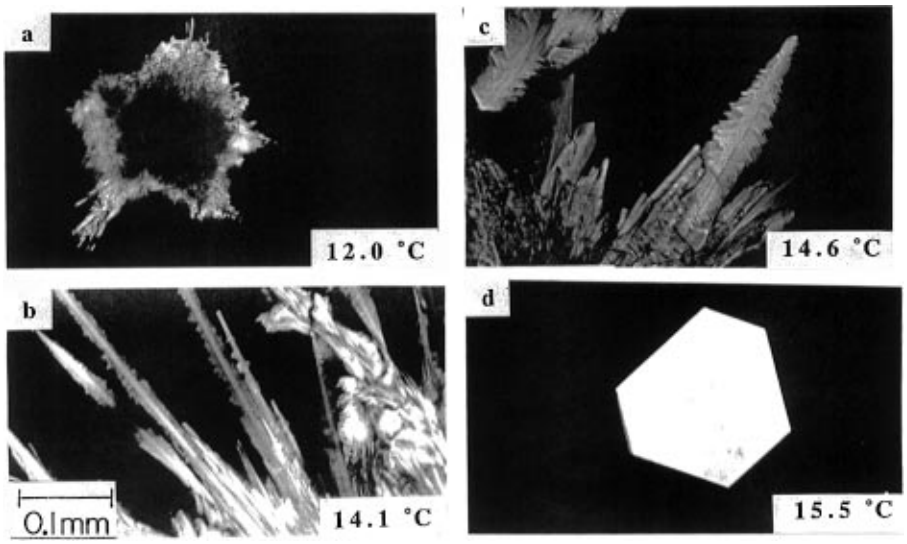

Figure 2. Temperature dependence of morphology.

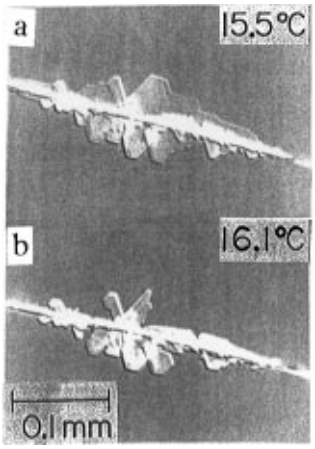

Figure 3. Melting behavior of the β phase.

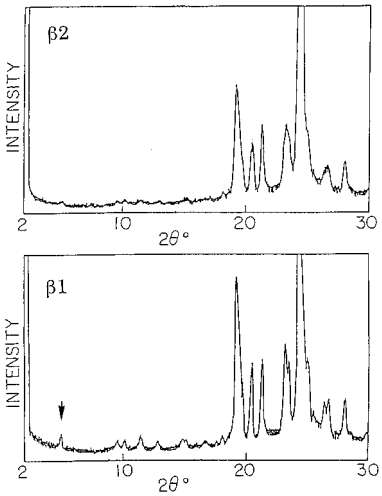

Figure 4. X-ray powder diffraction patterns of β_1 and β_2.

to some extent at 16.0 °C (Figure 3b). However, the rod and the early developed flat region did not melt at 16.0 °C but did at 16.3 °C. The crystal grown below 14.0 °C completely melted at 16.0 °C when the crystal was heated just after the crystallization. We found also that the β phase exhibited systematically two different values of the heat of fusion. For example, a specimen crystallized at 11.0 °C melts at about 15.9 °C and the heat of fusion ΔH_{fus} is 48.9 kJ/mol. On the other hand, a specimen crystallized at 15.5 °C melts at 16.3 °C and ΔH_{fus} is 51.9 kJ/mol. When a specimen grown below 14.0 °C is held at 15.5 °C, the melting point and the heat of fusion approach 16.3 °C and 51.9 kJ/mol, respectively, with increasing holding time.

Similar differences were observed in X-ray diffraction profiles, as shown in Figure 4. The specimen crystallized at 11.0 °C showed very weak reflections due to long spacings for $2\theta < 10°$. These reflections increased in intensity after standing at 15.5 °C for 2 days. Reflections in the region of $15 < 2\theta < 30°$ also became sharper with some of them being split into doublets. However, the overall diffraction pattern has not changed much.

From the above experimental results, we conclude that the β phase of oleic acid can be classified into two phases, β_1 (mp 16.3 °C) and β_2 (mp 16.0 °C). We have already reported a complex solution−crystallization mechanism of *n*-fatty acids accompanying a solid-state phase transition from a metastable phase to a stable phase.[19,20] We now infer that a similar phenomenon also takes place during the melt crystallization of the β phase, i.e., the stable phase β_1 was generated via a metastable state β_2. At first the crystal grows as the β_2 phase followed by the transformation of the β_2 phase to the β_1 phase through a solid-state phase transition. The observation that only a portion near the growing end melts at 16.0 °C (Figure 3) supports this interpretation. We therefore considered that the crystal grows as β_1 only in the vicinity of the melting point (16.3 °C).

Crystal Structure of β_1. The experimental conditions and the cell parameters are summarized in Table 1, and the coordinates of non-hydrogen atoms are listed in Table 2.

The γ phase of oleic acid has been typical of the crystal structure models for lipids and related compounds containing cis-unsaturated acyl groups. The features of the γ phase are the unit cell of pseudoorthorhombic system ($P2_1/a$), the *skew*−*cis*−*skew*′ type conformation of C−C═C−C portion, and the O′// subcell characteristic of cis-monounsaturated fatty acids. The structure of β_1 obtained is far different from that of γ in every respect, space group, layer structure, molecular conformation, and subcell.

The β_1 phase belongs to a triclinic system of space group $P\bar{1}$. The asymmetric unit contains two crystallographically different molecules, A and B. In other words, the unit cell contains two types of dimers (Figure 5). The bond lengths, bond angles, and dihedral angles of molecules A and B are summarized in Table 3.

TABLE 1: Crystallographic Data of Oleic Acid β_1 Phase

molecular formula	$C_{18}H_{34}O_2$
M_r	564.90
D_x	1.04 Mg m^{-3}
a (Å)	9.317(2)
b	5.543(2)
c	35.284(1)
α (deg)	87.90(3)
β	82.82(3)
γ	86.18(3)
F(000)	632
μ	0.499
cell volume (Å^3)	1803.1(8)
space group	$P\bar{1}$
molecules/unit cell	4
cell measurement temp	263 K
single crystals were obtained from acetonitrile	

TABLE 2: Fractional Coordinates of Non-H Atoms and Equivalent Isotropic Temperature Factors with Estimated Standard Deviations in Parentheses

$$B_{eq} = (8\pi^2/3)\sum_{i=1,3}\{\sum_{j=1,3}\{U_{ij}a^*_i a^*_j \vec{a}_i \cdot \vec{a}_j\}\}$$

atom	x	y	z	B_{eq}
AO1	−0.1752(2)	−0.0672(4)	0.022 26(6)	6.30(7)
AO2	0.0414(2)	−0.2472(4)	0.025 25(6)	6.36(7)
AC1	−0.0884(3)	−0.2365(5)	0.035 02(8)	4.64(8)
AC2	−0.1628(3)	−0.4127(6)	0.062 20(9)	5.06(9)
AC3	−0.0650(3)	−0.5877(6)	0.082 13(9)	4.77(9)
AC4	−0.1484(3)	−0.7428(6)	0.112 33(9)	4.71(8)
AC5	−0.0556(3)	−0.9243(6)	0.133 36(8)	4.51(8)
AC6	−0.1419(3)	−1.0690(6)	0.164 24(8)	4.63(8)
AC7	−0.0532(3)	−1.2571(6)	0.184 97(8)	4.45(8)
AC8	−0.1422(3)	−1.3987(6)	0.215 62(9)	5.11(9)
AC9	−0.0616(3)	−1.6008(5)	0.234 80(8)	4.92(8)
AC10	−0.1168(3)	−1.7296(5)	0.264 01(8)	4.92(8)
AC11	−0.2685(3)	−1.6962(6)	0.283 52(9)	4.97(9)
AC12	−0.3127(3)	−1.8855(5)	0.313 57(8)	4.35(8)
AC13	−0.4632(3)	−1.8323(5)	0.334 64(8)	4.54(8)
AC14	−0.5103(3)	−2.0187(5)	0.365 10(8)	4.53(8)
AC15	−0.6602(3)	−1.9602(6)	0.386 43(9)	4.73(8)
AC16	−0.7104(3)	−2.1477(5)	0.416 62(9)	4.81(8)
AC17	−0.8600(4)	−2.0854(7)	0.437 22(10)	5.87(10)
AC18	−0.9145(5)	−2.2746(9)	0.466 51(11)	7.33(13)
BO1	−0.5549(2)	−1.7213(4)	0.476 03(6)	5.98(7)
BO2	−0.3511(2)	−1.9529(4)	0.471 24(6)	6.02(7)
BC1	−0.4189(3)	−1.7705(5)	0.462 49(7)	4.55(8)
BC2	−0.3602(3)	−1.5853(6)	0.434 37(9)	4.92(9)
BC3	−0.2096(3)	−1.6495(5)	0.414 43(8)	4.57(8)
BC4	−0.1577(3)	−1.4588(5)	0.385 07(9)	4.61(8)
BC5	−0.0087(3)	−1.5188(5)	0.363 70(8)	4.44(8)
BC6	0.0389(3)	−1.3304(5)	0.333 49(8)	4.41(8)
BC7	0.1895(3)	−1.3801(5)	0.312 99(8)	4.37(8)
BC8	0.2336(3)	−1.1909(6)	0.282 86(9)	5.01(8)
BC9	0.3873(3)	−1.2187(5)	0.264 21(8)	4.69(8)
BC10	0.4425(3)	−1.0840(5)	0.235 81(8)	4.72(8)
BC11	0.3613(3)	−0.8809(6)	0.216 91(9)	4.94(9)
BC12	0.4493(3)	−0.7355(5)	0.186 91(8)	4.38(8)
BC13	0.3595(3)	−0.5449(5)	0.166 61(8)	4.40(8)
BC14	0.4459(3)	−0.3943(6)	0.136 45(8)	4.56(8)
BC15	0.3525(3)	−0.2153(6)	0.115 21(8)	4.65(8)
BC16	0.4372(3)	−0.0573(6)	0.085 48(8)	4.83(9)
BC17	0.3419(4)	0.1219(7)	0.064 70(10)	6.00(11)
BC18	0.4228(5)	0.2851(7)	0.035 80(10)	7.03(14)

The β_1 phase forms a unique interdigitated structure as shown in Figure 6. Usually, fatty acids form a segregated lamellar structure, where the methyl terminals are segregated from the carboxyl groups.[21−23] Therefore, their lamellar interfaces solely consist of methyl groups. The γ phase of oleic acid is a typical example of this segregated structure. On the other hand, the lamellar interfaces of the β_1 phase consist of methyl and carboxyl groups. In more detail, there are two types of interfaces; one interface consists of the methyl groups of molecule A and the carboxyl groups of molecule B; the other consists of the carboxyl groups of molecule A and the methyl groups of molecule B. This nonsegregated lamellar structure has not been found in other cis-unsaturated fatty acids. Only the A-super form[24,25] and the A1 form[26] of *n*-saturated fatty acids form a nonsegregated structure.

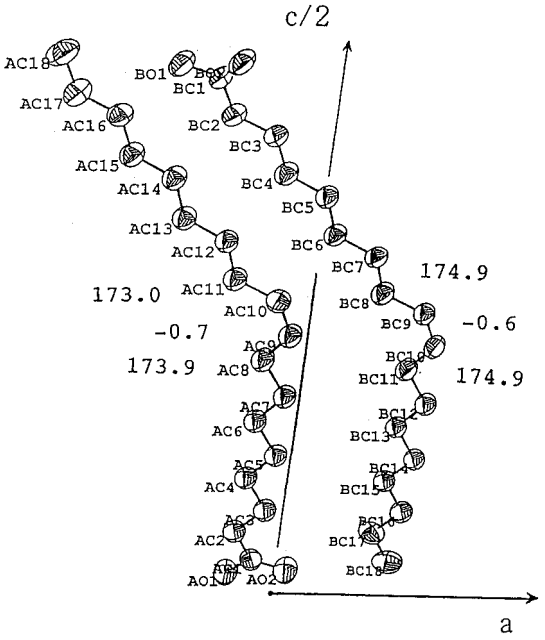

Figure 5. Two crystallographically different molecules of the β_1 phase in an asymmetric unit.

Another important point is the conformation around the carboxyl group. We have shown that the cis-olefin group of cis-unsaturated fatty acids can take various types of conformation.[27−30] The molecular mechanics calculation using MM2[31] on *cis*-3-hexene supports this conclusion.[12] The conformational energy does not depend very sensitively on dihedral angles of both C−C bonds linked to the cis-C=C bond. So far, we have found *skew*−*cis*−*skew* type (erucic acid $\gamma 1$ [28] and petroselinic acid high-melting phase[28]), *skew*−*cis*−*skew*′ (oleic and erucic acids γ[7,29]), and distorted *skew*−*cis*−*skew*′ (about 160, 0, and −160° in the petroselinic acid low-melting phase[30]). However, the conformations of molecules A and B are quite different from these conformations. The dihedral angles of the portion C(8)−C(9)=C(10)−C(11) are 173.9, −0.7, and 173.0° for molecule A and 174.9, −0.6, 174.9° for molecule B. Therefore, both molecules A and B can be regarded as *trans*−*cis*−*trans* type.

As shown in Figure 7, polymethylene chains form two types of the triclinic parallel subcell (T||), which are oriented in directions different from each other. One consists of the methyl side chains of molecule A and the carboxyl side chains of molecule B (subcell 1), and the other consists of the carboxyl side chain of molecule A and the methyl side chains of molecule B (subcell 2). The b_s axis of subcell 1 is parallel to the b axis of the main lattice, while the a_s and b_s axes of subcell 2 are not parallel to the basal (001) plane. There are systematic differences in subcell parameters between the two types of subcells, as listed in Table 4. The polymethylene chains incline toward the basal plane [(001) plane] by about 45° for both subcells 1 and 2. This inclination is rather large compared with those of *n*-fatty acids.

The plane of the carboxyl group (O−C=O plane) is almost coplanar with the carboxyl side polymethylene chains for both

TABLE 3: Selected Bond Lengths (Å), Bond Angles (deg), and Torsion Angles (deg)

selected bond lengths		selected bond angles		selected torsion angles	
AO1−AC1	1.302(0.003)	AO1−AC1−AO2	122.23(0.27)	9.08(0.47)	AO2−AC1−AC2−AC3
AO2−AC1	1.214(0.003)	AO2−AC1−AC2	123.73(0.27)	−171.03(0.28)	AO1−AC1−AC2−AC3
AC1−AC2	1.486(0.004)	AO1−AC1−AC2	114.04(0.27)	173.85(0.28)	AC1−AC2−AC3−AC4
AC2−AC3	1.503(0.004)	AC1−AC2−AC3	115.62(0.26)	179.72(0.29)	AC2−AC3−AC4−AC5
AC3−AC4	1.514(0.004)	AC2−AC3−AC4	112.38(0.25)	177.84(0.27)	AC3−AC4−AC5−AC6
AC5−AC6	1.510(0.004)	AC3−AC4−AC5	114.88(0.25)	178.21(0.30)	AC4−AC5−AC6−AC7
AC6−AC7	1.512(0.004)	AC4−AC5−AC6	113.37(0.24)	180.00(0.28)	AC5−AC6−AC7−AC8
AC7−AC8	1.508(0.004)	AC5−AC6−AC7	114.75(0.25)	175.14(0.29)	AC6−AC7−AC8−AC9
AC8−AC9	1.496(0.004)	AC6−AC7−AC8	113.55(0.25)	173.88(0.32)	AC7−AC8−AC9−AC10
AC9−AC10	1.303(0.004)	AC7−AC8−AC9	115.68(0.26)	−0.69(0.53)	AC8−AC9−AC10−AC11
AC10−AC11	1.496(0.004)	AC8−AC9−AC10	124.58(0.28)	172.96(0.31)	AC9−AC10−AC11−AC12
AC11−AC12	1.504(0.004)	AC9−AC10−AC11	125.35(0.27)	175.38(0.28)	AC10−AC11−AC12−AC13
AC12−AC13	1.519(0.004)	AC10−AC11−AC12	115.54(0.25)	−179.76(0.26)	AC11−AC12−AC13−AC14
AC13−AC14	1.509(0.004)	AC11−AC12−AC13	113.36(0.25)	178.90(0.28)	AC12−AC13−AC14−AC15
AC14−AC15	1.522(0.004)	AC12−AC13−AC14	114.53(0.25)	178.91(0.26)	AC13−AC14−AC15−AC16
AC15−AC16	1.515(0.004)	AC13−AC14−AC15	113.83(0.24)	−179.71(0.29)	AC14−AC15−AC16−AC17
AC16−AC17	1.514(0.004)	AC14−AC15−AC16	114.59(0.25)	177.94(0.29)	AC15−AC16−AC17−AC18
AC17−AC18	1.512(0.005)	AC15−AC16−AC17	113.42(0.27)	4.62(0.46)	BO2−BC1−BC2−BC3
BO1−BC1	1.312(0.003)	AC16−AC17−AC18	114.26(0.34)	−172.89(0.26)	BO1−BC1−BC2−BC3
BO2−BC1	1.207(0.003)	BO1−BC1−BO2	122.79(0.27)	177.82(0.26)	BC1−BC2−BC3−BC4
BC1−BC2	1.484(0.004)	BO2−BC1−BC2	123.98(0.27)	−178.57(0.27)	BC2−BC3−BC4−BC5
BC2−BC3	1.515(0.004)	BO1−BC1−BC2	113.18(0.28)	177.86(0.26)	BC3−BC4−BC5−BC6
BC3−BC4	1.512(0.004)	BC1−BC2−BC3	114.93(0.26)	177.42(0.28)	BC4−BC5−BC6−BC7
BC5−BC6	1.511(0.004)	BC2−BC3−BC4	112.59(0.25)	179.54(0.26)	BC5−BC6−BC7−BC8
BC6−BC7	1.510(0.004)	BC3−BC4−BC5	114.35(0.25)	174.39(0.28)	BC6−BC7−BC8−BC9
BC7−BC8	1.505(0.004)	BC4−BC5−BC6	113.54(0.24)	174.93(0.30)	BC7−BC8−BC9−BC10
BC8−BC9	1.500(0.004)	BC5−BC6−BC7	114.62(0.25)	−0.62(0.51)	BC8−BC9−BC10−BC11
BC9−BC10	1.301(0.004)	BC6−BC7−BC8	113.50(0.25)	174.91(0.31)	BC9−BC10−BC11−BC12
BC10−BC11	1.498(0.004)	BC7−BC8−BC9	115.69(0.25)	175.54(0.28)	BC10−BC11−BC12−BC13
BC11−BC12	1.500(0.004)	BC8−BC9−BC10	124.79(0.27)	179.51(0.27)	BC11−BC12−BC13−BC14
BC12−BC13	1.518(0.004)	BC9−BC10−BC11	124.79(0.27)	176.81(0.29)	BC12−BC13−BC14−BC15
BC13−BC14	1.512(0.004)	BC10−BC11−BC12	115.89(0.26)	178.47(0.27)	BC13−BC14−BC15−BC16
BC14−BC15	1.515(0.004)	BC11−BC12−BC13	113.57(0.25)	−179.60(0.30)	BC14−BC15−BC16−BC17
BC15−BC16	1.519(0.004)	BC12−BC13−BC14	114.64(0.24)	178.53(0.31)	BC15−BC16−BC17−BC18
BC16−BC17	1.517(0.004)	BC13−BC14−BC15	113.36(0.24)		
BC17−BC18	1.502(0.005)	BC14−BC15−BC16	114.30(0.25)		
BC15−BC16−BC17	113.56(0.27)				
BC16−BC17−BC18	114.83(0.34)				

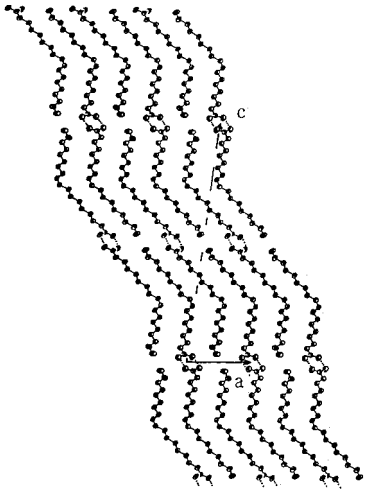

Figure 6. ORTEP view of the β_1 phase. Thermal ellipsoids are plotted at the 50% probability level.

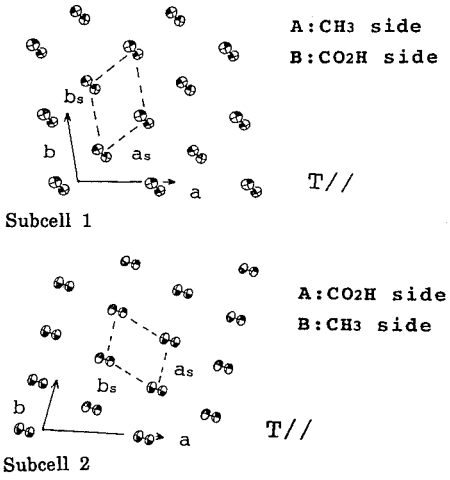

Figure 7. Two types of subcell structures and their orientations of oleic acid β_1.

molecules A and B. In this case, the C(3)−C(2)−C(1)═O group takes a cis or trans arrangement about the C(1)−C(2) bond as shown in Figure 8. Judging from the C−O bond lengths and the torsion angles about C(1)−C(2), the C(1)−O-(2) group should be assigned to the C═O group and the C(3)−C(2)−C(1)═O(2) portion takes the cis conformation in both molecules A and B. Some polymorphs of fatty acids show cis−trans tautomerism through simultaneous transfer of two hydrogen atoms.[32] It is considered that the hydrogen-bonded O···O distance is closely related to the occurrence of the cis−trans tautomerism.[33] The O···O distance is 2.634 Å for molecule A and 2.654 Å for molecule B. The former is rather smaller than the value found in the polymorphs where cis−trans tautomerism does not occur (2.67−2.68 Å).[30,34] There is a possibility of tautomerism at least for molecule A.

Discussion

1. Structure of the (001) Crystal Face. As described in the previous section, the β phase of oleic acid has a characteristic interdigitated structure. The intensity distribution of the (00*l*)

TABLE 4: Subcell Parameters

	subcell 1[a]	subcell 2[b]
a_s	4.09	4.18
b_s	5.36	5.54
c_s	2.54	2.54
α	81.4	72.2
β	106.5	109.7
γ	120.8	123.5
inclination of chains toward the (001) plane (deg)		
molecule A	45	45
molecule B	46	46

[a] This subcell is formed with the carboxyl side chains of A and the methyl side chains of B. [b] This subcell is formed with the methyl side chains of A and the carboxyl side chains of B.

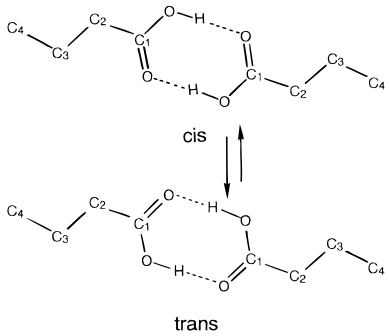

Figure 8. Cis and trans conformations of C(3)−C(2)−C(1)═O group.

reflections reflects this structure. Long-chain compounds usually exhibit a series of intense (00*l*) reflections. In this case, the strong intensities of the (00*l*) reflections of low orders of *l* are ascribed to the electron deficiency at the lamellar interface consisting of methyl terminals.[35] However, there is no such electron deficiency at the lamellar interfaces of oleic acid β, where both methyl groups and carboxyl groups are present.

Triglycerides containing a cis-unsaturated chain in the second position form a three-layered structure. It is assumed that cis-unsaturated acyl chains form a nonsegregated structure in the centered layer.[21−23] We consider that the structure of the β phase is helpful for the model building for the polymorphic phases of such mixed saturated and unsaturated triglycerides.

On the basis of this interdigitated structure, it could be inferred that the (001) crystal face of the β phase also forms a characteristic structure. The hydrogen bonding of fatty acids is so strong that it is natural that the molecules at the surface also take a dimer structure. If this expectation is correct, the population of molecules at the first surface layer is half as much as that in the inner layers. Furthermore, it can also be expected that there are two types of surface structures; one is formed with dimers of molecule A and the other with dimers of molecule B. The incidence of the two types of surfaces may depend on their surface energy. Because of the low density, the structure of the first layer probably exhibits a strong temperature dependence. At low temperatures the molecules may tend to form a dense structure, taking advantage of an increase of cohesive energy, and near the melting point the molecules may move to change the packing into a looser structure favoring higher entropy.

2. Possible Crystal Structure of β_2. Although the crystal structure of the β_2 phase has not been determined yet, we inferred that the β_2 phase has a strong structural resemblance to the β_1 phase on the basis of the following similarities in X-ray diffraction patterns (Figure 4).

(1) There is no intense reflection due to a lamellar structure in the low-angle region of $2\theta < 10°$.

(2) The positions of the weak reflections due to long spacings are almost the same as those of the β_1 phase. For instance, the (002) reflection was observed at about 5° in both β_1 and β_2.

(3) The intense reflections in the region of $18 < 2\theta < 30°$, which are due to the subcell structure, appear at almost the same position with similar relative intensity ratios.

It might be concluded that the β_2 phase also forms the interdigitated structure whose lamellar thickness is about the same as that of β_1 and that polymethylene chains are accommodated in the T|| subcell.

In this measurement, the peak width of the β_2 phase became sharper during a gradual transformation to the β_1 phase at 15.5 °C. It seems that some disorders have been incorporated into the β_2 specimen during the crystallization at a large supercooling of about 5 °C.

3. Possibility of Order−Disorder Transitions. Although there is a reversible order−disorder transition accompanying conformational disordering at the methyl side chains between the α and γ phases, the β phase does not show such a reversible transition. This characteristic can be easily understood with the crystal structure; a methyl terminal group is surrounded by carboxyl groups forming dimers with hydrogen bonds. Therefore, the conformational disordering at the methyl terminals needs a much larger activation energy in β than in the other polymorphs, leading to little possibility of transition.

4. Factors Affecting the Formation of Interdigitated Structures. We interpret the fact that the β phase has so far been found only in oleic acid as follows. Oleic acid only has the same number of carbon atoms between methyl and carboxyl side chains of natural cis-monounsaturated fatty acids. If there is a difference in chain length, the interdigitated structure should produce a void at the methyl terminal or carboxyl terminal. For example, the virtual β phase of palmitoleic acid (*cis*-9-hexadecenoic acid) has a void at the methyl terminals, which decreases the cohesive energy of the lattice. In the case of shorter carboxyl side chains, there is a void at the carboxyl terminals and hydrogen bonds cannot be formed. This is clearly an unfavorable structure. Therefore, the coincidence in the number of carbon atoms between methyl side and carboxyl side chains is a very important factor for the interdigitated structure.

5. Crystal Growth. As described in the Introduction, the rate of crystal growth of the β phase is unusually lower than that of the other polymorphic phases of long-chain compounds. Furthermore, the occurrence of the β phase is rare compared with the α and γ phases. In other words, the nucleation rate is also quite low.

On the basis of the crystal structure of the β phase, we infer that the following factors are the causes for the rareness of crystal occurrence and the low growth rate. One factor is the conformation of cis-olefin groups. As stated above, the conformation of this portion can be recognized as *trans*−*cis*−*trans* type. According to the molecular mechanics calculation, this conformation is less stable at least by 1.5 kcal/mol than the minimum energy.[12] To build a single crystal of β, a cluster should be formed where molecules take this unstable conformation. That is clearly a high-energy state. Therefore, the nucleation of β is energetically unfavorable. A similar discussion can be made for the process of crystal growth. A molecule that has attached to a crystal face should take the *trans*−*cis*−*trans* conformation in order to coalesce into the crystal face; this process may be energetically unfavorable and could be a bottleneck of the crystal growth.

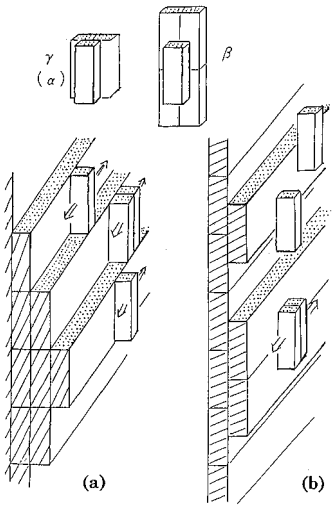

Figure 9. Schematic representation of the growing lateral face in the γ phase and the β phase.

The detailed information about the structure of the (001) face has not been obtained. However, from the crystal structure, the (001) face of β is unique; the density of molecular chains at the (001) face is one-half that of the interior of single crystals. In case of usual polymorphs of long-chain compounds, the average distance between nonbonded atoms is largest at the lamellar interface. The intermolecular interactions along the lamellar stacking direction are weak compared with those in the lateral direction. Therefore, the surface energy, i.e., energy necessary for forming a crystal face per unit area, takes a minimum value at the (001) face. In the case of the β phase where a molecule of a dimer penetrates into the next layer, the intermolecular interaction at the interface becomes much stronger, which may result in a large surface energy of the (001) face. The estimation of the surface energy is difficult at present, since it needs detailed information about the surface structure. However, it is reasonable to attribute one reason for the low nucleation and growth rates to the high surface energy of the crystal faces. It is well-known that the surface energy of the lamellar folding of polymer crystals is significantly larger than that of lateral faces, and therefore, the melt−crystallization of macromolecules needs a large supercooling.[36] For the melt crystallization of β, however, a large supercooling is not available because the nucleation and crystal growth of the α phase surpass those of the β phase.

Another important point is probably the structure of the growing crystal ends. For usual polymorphs of long-chain compounds, a growth unit (in the case of fatty acids, a dimer) newly attached at the growing crystal ends can be stabilized largely with dispersion forces from the lateral side of the crystal, as shown in Figure 9a. In particular, the contributions from the lamellae in the same level are quite large. A growth unit can be attached at almost any position of the growing lateral face. However, the situation of the β phase is quite different from that of other long-chain compounds, as shown in Figure 9b. In the β phase where the neighboring dimers are different in height by one molecular length, the number of potential sites suitable for the attachment of a new dimer decreases significantly. It seems that a flat site consisting of more than two lamellar layers (Figure 9, top; at least this site needs four dimers, in contrast with two dimers in the γ phase) is required for the adsorption and stabilization of a dimer; the whole part of the dimer can be incorporated into a crystal face in register and can get dispersion forces from the crystal wall. However, a flat site consisting of one lamellar layer cannot stabilize fully a newly attached dimer; only a half portion of the dimer can be stabilized, and the other one cannot attach steadily on the crystal face (this is a structure similar to the overhang that appears in crystallization under high supersaturation[37]). We inferred that these limited possibilities of positioning of molecular attachment would suppress the crystal growth rate.

Supporting Information Available: Tables of *F* data, anisotropic thermal factors, and coordinates of hydrogen atoms (13 pages). Ordering information is given on any current masthead page.

References and Notes

(1) Applegate, K. R.; Glomset, J. A. *J. Lipid Res.* **1991**, *32*, 1635, 1645.
(2) Pearce, L. L.; Harvey, S. C. *Biophys. J.* **1993**, *65*, 1084.
(3) Di. L.; Small, D. M. *J. Lipid Res.* **1993**, *34*, 1611.
(4) Di, L.; Small, D. M. *Biochemistry* **1995**, *34*, 16672.
(5) Suzuki, M.; Ogaki, T.; Sato, K. *J. Am. Oil Chem. Soc.* **1985**, *62*, 1600.
(6) Lutton, E. S. *Oil Soap (Chicago)* **1946**, *23*, 265.
(7) Abrahamsson, S.; Ryderstedt-Nahringbauer, I. *Acta Crystallogr.* **1962**, *15*, 1261.
(8) Kobayashi, M.; Kaneko, F.; Sato, K.; Suzuki, M. *J. Phys. Chem.* **1986**, *90*, 6371.
(9) Kobayashi, M. In *Crystallization and Polymorphism of Fats and Fatty Acids;* Garti, N., Sato, K., Eds.; Marcel Dekker: New York, 1988.
(10) Sato, K. In *Advance in Applied Lipid Research*; Padley, F., Ed.; JAI Press: New York, 1996; Vol. 2.
(11) Kaneko, F.; Yamazaki, K.; Kobayashi, M.; Sato, K.; Suzuki, M. *Spectrochim. Acta* **1994**, *94*, 3180.
(12) Kaneko, F.; Yamazaki, K.; Kobayashi, M.; Sato, K.; Suzuki, M. *J. Phys. Chem.* **1996**, *100*, 9138.
(13) Sato, K.; Yano, Y.; Kawada, I.; Kawano, M.; Kaneko, F.; Suzuki, M. *J. Am. Oil Chem. Soc.*, submitted.
(14) Yoshimoto, N. Doctoral Thesis, Hiroshima University, Hiroshima, Japan, 1991.
(15) Kaneko, F.; Sigenaga, O.; Kitagawa, K.; Kobayashi, M.; Furukawa, Y.; Sato, K.; Suzuki, M. To be published.
(16) Sheldrick, G. M. *SHELXS93*; University of Goetingen: Goetingen, Germany, 1993; program for crystal structure solution.
(17) Sheldrick, G. M. *SHELXS86*; University of Goetingen: Goetingen, Germany, 1986; program for crystal structure solution.
(18) Johnson, C. K. ORTEP II, revised. Report ORNL-3794; Oak Ridge National Laboratory: Oak Ridge, TN, 1971.
(19) Kaneko, F.; Shimofuku, T.; Miyamoto, H.; Kobayashi, M.; Suzuki, M. *J. Phys. Chem.* **1992**, *96*, 10554.
(20) Kaneko, F.; Sakashita, H.; Kobayashi, M. *J. Phys. Chem.* **1994**, *98*, 3801.
(21) Small, D. M., Ed. *The Physical Chemistry of Lipids*; Plenum: New York, 1986.
(22) Larsson, K. In *The Lipid Handbook*; Gunstone, F. D., Harwood, J. L., Padley, F. B., Eds.; Chapman and Hall: London, 1988.
(23) Kobayashi, M.; Kaneko, F. *J. Dispersion Sci. Tecnol.* **1989**, *10*, 319.
(24) von Sydow, E. *Acta Chem. Scand.* **1956**, *10*, 1 .
(25) Goto, M.; Asada, E. *Bull. Chem. Soc. Jpn.* **1978**, *51*, 70.
(26) Lomer, T. R. *Acta Crystallogr.* **1963**, *16*, 984.
(27) Kaneko, F.; Kobayashi, M.; Kitagawa, Y.; Matsuura, Y.; Sato, K.; Suzuki, M. *Acta Crystallogr.* **1992**, *C48*, 1060.
(28) Kaneko, F.; Kobayashi, M.; Kitagawa, Y.; Matsuura, Y.; Sato, K.; Suzuki, M. *Acta Crystallogr.* **1992**, *C48*, 1057.
(29) Kaneko, F.; Yamazaki, Y.; Kobayashi, M.; Kitagawa, Y.; Matsuura, Y.; Sato, K.; Suzuki, M. *Acta Crystallogr.* **1993**, *C49*, 1232.
(30) Kaneko, F.; Kobayashi, M.; Kitagawa, Y.; Matsuura, Y.; Sato, K.; Suzuki, M. *Acta Crystallogr.* **1992**, *C48*, 1054.
(31) Allinger, N. *L. J. Am. Chem. Soc.* **1977**, *99*, 8127.
(32) Hayashi, S.; Umemura, J. *J. Chem. Phys.* **1975**, *63*, 1732.
(33) Matsushita, E.; Matsubara, T. *Prog. Theor. Phys.* **1982**, *6*, 1.
(34) Kaneko, F.; Kobayashi, M.; Kitagawa, Y.; Matsuura, Y. *Acta Crystallogr.* **1990**, *C46*, 1490.
(35) Strobl, G.; Ewen, B.; Fischer, E. W.; Piesczek, W. *J. Chem. Phys.* **1974**, *61*, 5257.
(36) Sperling, L. H. *Introduction to Physical Polymer Science;* John Wiley & Sons: New York, 1986.
(37) Sato, K. *Jpn. J. Appl. Phys.* **1980**, *19*, 1257.